

EUR Research Information Portal

Gray matter involvement in radiologically isolated syndrome

Published in:

Medicine (United States)

Publication status and date:

Published: 01/01/2016

DOI (link to publisher):

[10.1097/MD.0000000000003208](https://doi.org/10.1097/MD.0000000000003208)

Document Version

Publisher's PDF, also known as Version of record

Document License/Available under:

CC BY

Citation for the published version (APA):

Labiano-Fontcuberta, A., Mato-Abad, V., Álvarez-Linera, J., Hernández-Tamames, J. A., Martínez-Ginés, M. L., Aladro, Y., Ayuso, L., Domingo-Santos, A., & Benito-León, J. (2016). Gray matter involvement in radiologically isolated syndrome. *Medicine (United States)*, 95(13), e3208. <https://doi.org/10.1097/MD.0000000000003208>

[Link to publication on the EUR Research Information Portal](#)

Terms and Conditions of Use

Except as permitted by the applicable copyright law, you may not reproduce or make this material available to any third party without the prior written permission from the copyright holder(s). Copyright law allows the following uses of this material without prior permission:

- you may download, save and print a copy of this material for your personal use only;
- you may share the EUR portal link to this material.

In case the material is published with an open access license (e.g. a Creative Commons (CC) license), other uses may be allowed. Please check the terms and conditions of the specific license.

Take-down policy

If you believe that this material infringes your copyright and/or any other intellectual property rights, you may request its removal by contacting us at the following email address: openaccess.library@eur.nl. Please provide us with all the relevant information, including the reasons why you believe any of your rights have been infringed. In case of a legitimate complaint, we will make the material inaccessible and/or remove it from the website.

Gray Matter Involvement in Radiologically Isolated Syndrome

Andrés Labiano-Fontcuberta, MD, PhD, Virginia Mato-Abad, PhD, Juan Álvarez-Linera, MD, PhD, Juan Antonio Hernández-Tamames, PhD, M² Luisa Martínez-Ginés, MD, PhD, Yolanda Aladro, MD, PhD, Lucía Ayuso, MD, PhD, Ángela Domingo-Santos, MD, and Julián Benito-León, MD, PhD

Abstract: The unanticipated magnetic resonance imaging (MRI) detection in the brain of asymptomatic subjects of white matter lesions suggestive of multiple sclerosis has recently been named as radiologically isolated syndrome (RIS). The pathophysiological processes of RIS remain largely unknown and questions as to whether gray matter

alterations actually occur in this entity are yet to be investigated in more detail. By means of a 3 T multimodal MRI approach, we searched for cortical and deep gray matter changes in a cohort of RIS patients. Seventeen RIS patients, 17 clinically isolated syndrome (CIS) patients (median disease duration from symptom onset = 12 months), and 17 healthy controls underwent MRI and neuropsychological testing. Normalized deep gray matter volumes and regional cortical thickness were assessed using FreeSurfer. SIENAX was used to obtain normalized global and cortical brain volumes. Voxelwise morphometry analysis was performed by using SPM8 software to localize regions of brain tissue showing significant changes of fractional anisotropy or mean diffusivity. Although no differences were observed between CIS and healthy controls groups, RIS patients showed significantly lower normalized cortical volume (673 ± 27.07 vs 641 ± 35.88 [$\text{cm}^3 \times 10^3$], Tukey P test = 0.009) and mean thalamic volume (0.0051 ± 0.4 vs 0.0046 ± 0.4 mm, $P = 0.014$) compared with healthy controls. RIS patients also showed significant thinning in a number of cortical areas, that were primarily distributed in frontal and temporal lobes ($P < 0.05$, uncorrected). Strong correlations were observed between T2-white matter lesion volume and regional cortical thickness (rho spearman ranging from 0.60 to 0.80). Our data suggest that white matter lesions on T2-weighted images are not the only hallmark of RIS. Future longitudinal studies with larger samples are warranted to better clarify the effect of RIS-related white matter lesions on gray matter tissue.

Editor: Massimo Tusconi.

Received: February 7, 2016; revised and accepted: March 7, 2016.

From the Department of Neurology, University Hospital "12 de Octubre" (AL-F, AD-S, JB-L); Neuroimaging Laboratory, Center for Biomedical Technology, Rey Juan Carlos University, Móstoles (VM-A, JAH-T); Department of Radiology, Hospital Ruber Internacional, Madrid, Spain (JA-L); Department of Neurology, University Hospital "Gregorio Marañón", Madrid (MLM-G); Department of Neurology, University Hospital of Getafe, Getafe (YA) Department of Neurology, University Hospital "Príncipe de Asturias", Alcalá de Henares (LA); Centro de Investigación Biomédica en Red sobre Enfermedades Neurodegenerativas (CIBERNED), Spain (JB-L); and Department of Medicine, Complutense University (JB-L), Madrid, Spain.

Correspondence: Julián Benito-León, MD, PhD, Avda. de la Constitución 73, portal 3, 7° Izquierda, E-28821 Coslada, Madrid, Spain (e-mail: jbenitol67@gmail.com).

Authors' contributions: AL-F (gandilabiano@hotmail.com) collaborated in: the conception, organization and execution of the research project; the statistical analysis design; and the writing of the manuscript first draft and the review and critique of the manuscript.

VM-A (virginia.mato@urjc.es) collaborated in: the conception, organization of the research project, and the review and critique of the manuscript.

JÁ-L (jalinera@ruberinternacional.es) collaborated in: the conception, organization of the research project, and; the review and critique of the manuscript.

JAH-T (juan.tamames@urjc.es) collaborated in: the conception, organization of the research project, and; the review and critique of the manuscript.

MLM-G (marisamgines@hotmail.com) collaborated in: the conception, organization of the research project, and the review and critique of the manuscript.

YA (yolanda.aladro@salud.madrid.org) collaborated in the conception, organization of the research project, and the review and critique of the manuscript.

LA (layusoperalta@gmail.com) collaborated in the conception, organization of the research project, and the review and critique of the manuscript.

AD-S (gela_yo@hotmail.com) collaborated in: the conception, organization of the research project, and the review and critique of the manuscript.

JB-L (jbenitol67@gmail.com) collaborated in: the conception, organization of the research project, and the review and critique of the manuscript.

This research was supported by Teva neuroscience and FEDER funds. JB-L is supported by the National Institutes of Health, Bethesda, MD, USA (NINDS #R01 NS39422), the Commission of the European Union (grant ICT-2011-287739, NeuroTREMOR), the Ministry of Economy and Competitiveness (grant RTC-2015-3967-1, NetMD—Platform for the tracking of movement disorders), and the Spanish Health Research Agency (grant FIS PI12/01602). We acknowledge the neuropsychologists Verónica Puertas, Yolanda Higuera, and Marta Cerezo for their assistance with the project.

The authors have no funding and conflicts of interest.

Copyright © 2016 Wolters Kluwer Health, Inc. All rights reserved.

This is an open access article distributed under the Creative Commons Attribution License 4.0, which permits unrestricted use, distribution, and reproduction in any medium, provided the original work is properly cited. ISSN: 0025-7974

DOI: 10.1097/MD.0000000000003208

(*Medicine* 95(13):e3208)

Abbreviations: ANOVA = Analysis of variance, CIS = Clinically isolated syndrome, DTI = Diffusion tensor imaging, DWI = Diffusion-weighted image, EDSS = Expanded Disability Status Scale, MRI = Magnetic resonance imaging, MS = multiple sclerosis, RIS = radiologically isolated syndrome, SD = standard deviation, WAIS-III = Wechsler Adult Intelligence Scale—Third Edition.

INTRODUCTION

The steady increase in the use of magnetic resonance imaging (MRI) for the evaluation of medical conditions, such as headaches or dizziness, has led to the emergence of a new condition named radiologically isolated syndrome (RIS), which is characterized by incidental brain MRI finding of white matter lesions demonstrating dissemination in space in subjects with a normal neurologic examination, and without historical accounts of typical multiple sclerosis (MS) symptoms.¹

A number of recent studies suggest that RIS and MS patients share both nonmotor clinical features²⁻⁵ and quantitative brain tissue damage,⁶⁻¹⁰ thereby suggesting that RIS, as an entity, reflects the earliest and preclinical form of MS. In line with this assumption, approximately one-third of RIS patients, mainly those with spinal cord involvement, are at higher risk for future symptomatic demyelinating event within 5 years.¹¹

There are too many unanswered questions regarding this entity, with the current impossibility of clarifying whether the observed white matter changes reflect the earliest stage of MS, a nondisabling form of MS, or even a different pathological condition. Furthermore, RIS quantitative MRI studies to date have either included a meaningful proportion of RIS patients with markers of evolution to future MS,^{6,8,12} and as a consequence, their results might not be entirely extrapolable to the general RIS population, or have compared RIS patients with MS patients^{3,8,12} rather than with CIS patients who potentially might have a closer biologic and pathological similarity with RIS patients.

The great uncertainty over the true morphological changes in brain with RIS underlines the necessity of additional comprehensive studies with multimodal structural brain imaging analyses. Until now, no study has been conducted to compare the brain damage occurring beyond T2 visible lesions between RIS and CIS patients. The comparison of a group of RIS patients with a CIS group without high disease activity who have not converted to definite MS has the potential advantage to directly contrast 2 groups with a closer stage disease.

In this context, the present study used a multimodal 3 T MRI approach aimed to evaluate the differences in cortical thickness, cortical and subcortical gray matter volume, and white matter integrity between RIS, CIS, and healthy volunteers; assess to what extent RIS quantitative brain measures share similarities or differences with those of CIS patients; analyze the correlation between specific brain changes with cognitive and psychiatric symptoms of RIS patients.

METHODS

Study Design and Subjects

Seventeen RIS subjects, most of whom came from already existing MS databases, were recruited at 4 centers specialized in demyelinating diseases in Madrid (Spain). These subjects had come to our attention after undergoing conventional brain 1.5 T MRI for various medical events not suggestive of MS. All 1.5 T MRI examinations included axial fluid-attenuated inversion recovery, fast spin echo, and T2- and T1-weighted without and with gadolinium in axial, coronal, and sagittal planes of view. Brain white matter abnormalities were initially identified by a neuroradiologist and subsequently examined by an MS specialist at each clinical site to guarantee they fulfilled the Okuda MRI criteria for RIS,¹ which imply the presence of white matter abnormalities suggestive of a demyelinating process (ovoid, well-circumscribed, and measuring $>3 \text{ mm}^2$) that satisfied Barkhof criteria (at least 3 of 4 criteria) for dissemination in space^{13,14}; not better accounted for by other disease processes, such as, in particular, vascular disease; and no apparent impact on everyday functioning.

After the initial MRI imaging, all RIS patients underwent cervical spinal MRI, but only a subgroup (50%) agreed to undergo lumbar puncture for CSF analysis. An extensive neurologic examination and an accurate clinical history were performed by neurologists with expertise in MS (AL-F, MLM-G, YA, LA, AD-S, and JB-L) to rule out both any neurologic sign and history of remitting clinical symptoms lasting $>24 \text{ h}$ consistent with MS. In addition, they underwent a complete nonstandardized workup (sedimentation rate, anticardiolipin antibody screen, antineutrophil cytoplasmic antibodies, anti-nuclear antibodies, Borrelia and syphilis serologies, rheumatoid factor, serum angiotensin-converting enzyme, thyroid function

studies, and vitamin B12 level) to rule out other medical conditions that could explain the observed lesions on brain MRI.

Seventeen patients who had presented with a CIS suggestive of MS were recruited from the University Hospital “Gregorio Marañón,” and from the University Hospital of Getafe, both in Madrid (Spain). Although the frequency of follow-up MRI examinations in CIS patients was slightly different across participating centers, all CIS patients underwent 1.5 T MRI examination (axial fluid-attenuated inversion recovery, fast spin echo, and T2- and T1-weighted without and with gadolinium in axial, coronal and sagittal planes of view) and a complete neurologic evaluation, including Expanded Disability Status Scale (EDSS)¹⁵ by experienced neurologists (MLM-G and YA). Dissemination in space and dissemination in time were evaluated according to the McDonald 2010 criteria.¹⁶ Patients selected met the following inclusion criteria: single clinical episode indicative of MS; total follow-up time of at least 3 months from the occurrence of the first inflammatory demyelinating event; and the presence of ≥ 1 asymptomatic T2 lesion(s) in at least ≥ 2 brain locations considered characteristic for MS (juxtacortical, periventricular, infratentorial, and spinal cord)¹⁷ at the initial or follow-up MRI. Participants were excluded if they had received steroid medication during the month before the study inclusion and a longitudinal evaluation >5 years.

We excluded RIS or CIS patients with history of alcohol or drug abuse, major acute comorbidities, or any major serious chronic illness 1 year before inclusion (patients with a stable chronic medical conditions were included).

RIS or CIS patients were matched for age, sex, and education with a control group consisting of 17 healthy controls (14 women, 3 men; mean age 42 years, range 27–56 years) with no history of known psychiatric or neurological disorders, which was recruited either from relatives or friends from health professionals at the University Hospital “12 de Octubre” of Madrid (Spain).

Once the study was described to subjects and written (signed) informed consent was obtained from all enrollees, a multisequence MRI examination was acquired in a single session using a single 3 T scanner at CIEN (Center for Research on Neurological diseases, in Spanish) Foundation in Madrid (Spain). Psychiatric and neuropsychological tests were conducted in a single session by experienced clinical neuropsychologists (VP; YH, MC, see acknowledgements) who were blinded to the clinical status during an interview during the week in which they had completed the aforementioned MR examination.

All procedures were approved by the ethical standards committees on human experimentation at the University Hospital “12 de Octubre” (Madrid).

Measurement Instruments

Cognitive functioning was performed through the Rao Brief Repeatable Battery.¹⁸ The Stroop test was administered to evaluate executive functions.¹⁹ Participants also completed the Vocabulary and Matrix subtests from the Wechsler Adult Intelligence Scale—Third Edition (WAIS-III).²⁰ Vocabulary subtest was used as a measure of crystallized intelligence, which is influenced by educational experience. Vocabulary scores have been suggested as a more reliable measure of cognitive reserve than demographic information (education and occupation),²¹ as some patients may have actually greater cognitive reserve through lifelong habits (ie, reading, writing,

and high-demand activities) and often surpass patients who may have more years of formal education. Matrix substest was used to measure fluid intelligence as it requires the ability to solve novel problems with minimal dependence on previously acquired knowledge.

Depression severity was measured by the original 17-item version of the Hamilton Depression Rating Scale.²²

MRI Acquisition

All MRI data were acquired with a clinical 3 T Signa HDx MRI scanner (GE Healthcare, Waukesha, WI) using an 8-channel phased array coil. The imaging (MRI) standardized protocol (without injection of contrast agent) included a 3D T1-weighted SPGR with a TR = 10.012 ms, TE = 4.552 ms, TI = 600 ms, NEX = 1, acquisition matrix = 288 × 288, full brain coverage, resolution = 0.4688 × 0.4688 × 1 mm, flip angle = 12.

The diffusion-weighted image (DWI) protocol acquisition consisted of 3 images without diffusion gradients ($b = 0$ s/mm²) followed by 45 images measured with 45 directions ($b = 1000$ s/mm²) isotropically distributed in space. Additional parameters of the acquisition were: TE = 85.3 ms, TR = 10.100 ms, flip-angle = 90, slice thickness = 3 mm (no gap), resolution = 2.6042 × 2.6042 × 2.6 mm, FOV = 250 mm and axial acquisition.

Data Post-processing

MRI

Cortical thickness and cortical volume measurements were calculated using the freely available software FreeSurfer (<http://surfer.nmr.mgh.harvard.edu/>). Using a surface-based approach, FreeSurfer can automatically segment the brain into different cortical regions of interest, and calculate average thickness in the defined regions. In brief, images underwent preprocessing including intensity normalization and skull stripping, which was followed by labeling of cortical and subcortical regions. FreeSurfer's main cortical reconstruction pipeline begins with registration of the structural volume with the Talairach atlas.²³ After bias field estimations and the removal of bias, the skull is stripped and subcortical white and gray matter structures were segmented.²⁴ Next, tessellation, automated topology correction, and surface deformation routines create white/gray (white) and gray/cerebrospinal fluid (pial) surface models.²⁵ These surface models were then inflated, registered to a spherical atlas, and used to parcellate the cortical mantle according to gyral and sulcal curvature.²⁶ The closest distance from the white surface to the pial surface at each surface's vertex was defined as the thickness.²⁶ Average cortical thickness, surface area, and total volume statistics corresponding to each parcellated region could then be computed. The accuracy of FreeSurfer's results was then assessed visually for the different subjects.

DWI

DWI data were preprocessed with FMRIB's Diffusion Toolbox (<http://fsl.fmrib.ox.ac.uk/fsl/fslwiki/FslOverview/>). Preprocessing consisted of eddy-current correction, motion correction, and the removal of non-brain tissue using the robust Brian Extraction Tool.²⁷ Diffusion tensor images (DTIs) were created using the weighted least squares fitting method. We derived images of fractional anisotropy or mean diffusivity from the DTI. To calculate the specific fractional anisotropy or mean diffusivity values in the subcortical regions, we need to map the DTI space to the FreeSurfer's structural space

(described above). The fractional anisotropy or mean diffusivity maps were resampled by means of a rigid-body transformation from the diffusion to the structural space. After that, the fractional anisotropy or mean diffusivity mean and standard deviation values from the FreeSurfer's subcortical regions were computed.

In addition, a voxel-based analysis pipeline was used to find differences in fractional anisotropy or mean diffusivity between groups. Voxel-based analysis of fractional anisotropy or mean diffusivity images were carried out with SPM8 software (www.fil.ion.ucl.ac.uk/spm/software/spm8/). First, b0 images were manually aligned to the anterior commissure-posterior commissure line, and the same alignment was applied to the fractional anisotropy or mean diffusivity images. Then, these fractional anisotropy images were coregistered to a fractional anisotropy template from FMRIB's Software Library using linear affine registration with normalized mutual information as the fitness function.²⁸ The same spatial transformation was applied to the mean diffusivity maps. The registered images were normalized to the fractional anisotropy template using a nonlinear registration algorithm²⁹ and were then smoothed with an 3D Gaussian kernel (4-mm full-wide half maximum). The spatial transformation was again applied to the mean diffusivity maps.

White Matter Lesion Volume Analysis

Study images were assessed by an experienced neuroradiologist (JA-L) who was unaware of participant clinical status. T2 hyperintense lesions were segmented in fluid-attenuated inversion recovery images by employing the automated lesion growth algorithm³⁰ as implemented in the LST toolbox version 2.0.11 (www.statisticalmodelling.de/lst.html) for SPM. Lesion masks were estimated and then transformed into standard space and averaged to yield a mean lesion mask across subjects.

Brain Volume Analysis

Normalized brain volumes were quantified on high-resolution T1-weighted image using the SIENAX method, part of the FMRIB Software Library.³¹

Statistical Analysis

The data were conducted using the SPSS Version 21.0 (SPSS, IBM Corporation, Chicago, IL). All tests were 2-sided, and significance was accepted at 5% level ($\alpha = 0.05$). Regional cortical thickness analyses were exploratory in nature and thus we consider that the application of Bonferroni correction for multiple comparisons analysis ($P < 0.05/33$ number of comparisons in each hemisphere) would overcorrect for type I error, especially in view of the insufficient power derived from the small sample size. Therefore, the present study presents those regional cortical thickness results with a significance level $P < 0.05$ uncorrected. Nevertheless, since the probability of false-positive results is higher than the standard alpha value, the conclusions are based exclusively on criteria such as the magnitude and the impact of the differences (eg, number of patients who are at least 2 standard deviations [SDs] below the mean) rather than the P value.

Using the Shapiro-Wilk test, we determined that all variables except T2 white matter lesion volume were normally distributed (Shapiro-Wilk test, $P > 0.05$). To analyze the correlation among radiological measures (brain volumes, cortical thickness), and clinical parameters or T2 white matter lesion

volume (not normally distributed), Pearson and Spearman coefficients were used respectively.

A general linear model analysis of variance (ANOVA) was applied to determine statistically significant differences between the groups for the continuous variables. Age, sex, and educational level were included as covariates as they can contribute to cortical thickness.³² Homogeneity of variances assumption was not met (Levene test <0.05) for deep gray matter comparisons and therefore Welch F test was the approach for performing the ANOVA analysis, followed by post-hoc Games Howell test for mean pairwise comparison analyses. For the categorical variables, the k-independent samples Kruskal-Wallis test was applied with post-hoc analysis for Mann-Whitney *U* tests.

Differences in fractional anisotropy or mean diffusivity between groups were obtained by performing a voxel-based analysis by means of the general linear model, with age and sex as covariates. We tested the significance of any observed differences using a paired *t* test with $P < 0.001$.

RESULTS

Sample Characteristics

Table 1 summarizes the demographic and clinical characteristics of the entire sample and shows that the groups were well-matched for age ($F[2,48]=0.68$, $P=0.51$), sex ratio ($\chi^2=0.55$, $P=0.75$), and educational level ($\chi^2=0.08$, $P=0.95$). Reasons for the first RIS patients MRI, which was performed a mean of 4.07 years (range 1–11) earlier, were: headache ($N=5$), dizziness ($N=4$), tinnitus-hypocusia ($N=3$), syncope ($N=1$), restless legs ($N=1$), research control ($N=1$), traffic accident ($N=1$), and prolactinoma ($N=1$).

The RIS patients were stratified into RISK+ (higher risk for conversion to future MS) versus RISK- (lower risk for conversion to future MS) according to the presence of lesions within the spinal cord or no lesions of the spinal cord, but presence of at least 2 of the following characteristics: abnormal cerebrospinal fluid, gadolinium enhancing lesions, or dissemination in time. Among the 6 RIS subjects who were classified as RISK+, 4 were included based on spinal cord lesions criteria and 2 on the presence of several risk criteria for conversion to MS. No RIS patients were being treated with disease-modifying therapies.

CIS patients were characterized by low clinical disability (median EDSS score of 0, range 0–4) and a relatively short duration of disease (median disease duration from clinical onset = 12 months). Only 3 of 17 (17.6%) CIS patients had a disease evolution from clinical onset <12 months, whereas 7 of 17 (41.1%) had a disease duration from symptom onset of at least 48 months. Of the 17 CIS patients, 5 (29.4%) presented with spinal cord symptoms, 4 (23.5%) with optic neuritis, 3 (17.6%) with brainstem symptoms, 3 with polysymptomatic onset, and 2 (11.8%) with hemispheric cerebral symptoms. All CIS subjects fulfilled dissemination in space according to the McDonald 2010 criteria.¹⁶ Of the 17 CIS patients, only 4 (23.5%) were treated with disease-modifying therapies (interferon beta-1a).

Eight (47.1%) RIS patients failed in at least one cognitive test, defined as a Z score ≤ 2.0 SD below the healthy controls mean of any of the cognitive tests, whereas 2 (11.8%) RIS patients failed in at least 2 cognitive tests, proportions virtually identical to those observed in CIS patients (47.1% and 5.9% respectively).

Using a cutoff score of 8 on the Hamilton Depression Rating Scale total score,²² 9 (52.9%) of the RIS group had at

least mild clinical depression, with more than half of them ($N=5$, 55.9%) having moderate depressive symptoms, rates identical to that observed among CIS patients.

Whole-brain Volume Analysis

Normalized cortical volumes were statistically different between groups as determined by ANOVA ($F[2,48]=5.22$, $P=0.009$). Normalized cortical volume was significantly lower on RIS group compared with healthy controls (673 ± 27.07 vs 641 ± 35.88 ($\text{cm}^3 \times 10^3$), Tukey P test = 0.009), whereas near-significant difference was observed between CIS and healthy control groups (648 ± 27.34 vs 673 ± 27.07 ($\text{cm}^3 \times 10^3$), Tukey P test = 0.057). A considerable trend toward significance in total brain volume was observed in RIS patients compared with healthy controls (1528 ± 64.40 vs 1575 ± 36.82 , $P=0.054$). Normalized total gray matter and white matter volumes were not statistically different between groups ($F=2.10$, $P=0.13$ and $F=0.94$, $P=0.40$, respectively). No differences between RISK- and RISK+ were detected. A trend toward lower normalized total brain and cortical volumes was observed in RIS patients who failed in at least one cognitive test compared with those without cognitive impairment, but these differences did not reach statistical significance ($P=0.12$ and 0.33 , respectively). No significant differences were found when RIS patients were subdivided according to the presence/absence of clinically significant depression (data not shown).

White matter lesion volume did not differ significantly between RIS and CIS groups as determined by Mann-Whitney *U* test ($P=0.13$). T2-white matter lesion volume was correlated with normalized cortical volume ($r=-0.59$, $P=0.012$) and normalized grey matter volume ($r=-0.52$, $P=0.03$) in RIS patients. Among CIS patients, correlations were seen between T2-white matter lesion volume and normalized gray matter volume ($r=-0.56$, $P=0.020$), normalized brain volume ($r=-0.51$, $P=0.038$), and normalized cortical volume ($r=-0.49$, $P=0.045$).

Deep Gray Matter and Cerebellar Volumes

Between-groups comparisons on deep gray matter and cerebellum volumes are shown in Table 2. Significant group difference was found between groups with regard to thalamic volume (F Welch $[2,30]=4.61$, $P=0.018$). Post-hoc Games-Howell test indicated that this difference was because of a difference between healthy controls versus RIS (Games-Howell, $P=0.014$). There were no other statistically significant differences between group means as determined by ANOVA Welch F test ($P > 0.10$ for all).

Among RIS patients, no correlations were found between mean thalamic volume and T2-white matter lesion volume ($r=-0.31$, $P=0.21$), normalized brain ($r=0.42$, $P=0.09$) or normalized cortical volume ($r=0.45$, $P=0.06$).

Cortical Thickness

Compared with healthy controls, RIS patients showed significant thinning in a number of cortical areas, that were primarily distributed in frontal and temporal lobes ($P < 0.05$, uncorrected). The extent of regional cortical thinning differed between the hemispheres, with most regions having the highest thinning in the right hemisphere. A single-subject analysis showed that right temporal lobe was particularly affected, as cortical thickness was at least 2 SDs below the healthy controls mean in the 47.1% of RIS subjects. Lateral orbitofrontal, transverse temporal gyrus, and posterior cingulate

TABLE 1. Demographic and Clinical Characteristics of the Sample

	Healthy Controls (N = 17)	Clinically Isolated Syndrome Patients (N = 17)	All Patients (N = 17)	RISK – (N = 11)	RISK+ (N = 6)
Female/male (ratio)	13/5 (2.6)	12/5 (2.4)	13/4 (3.2)	9/3 (3.0)	4/2 (2.0)
Age in years	42.0 ± 6.38 (27–56)	39.5 ± 6.1 (30–55)	41.6 ± 7.1 (27–52)	40.7 ± 6.4 (27–50)	43.6 ± 8.2 (29–52)
Educational level					
Primary school	2 (11.8%)	5 (29.4%)	4 (23.5%)	2 (18.2%)	2 (33.3%)
Secondary school	10 (58.8%)	4 (23.5%)	7 (41.2%)	6 (54.5%)	1 (16.7%)
University studies	5 (29.4%)	8 (47.1%)	6 (35.3%)	3 (27.3%)	3 (50%)
Mean age at RIS diagnosis	—	—	37.7 ± 7.4	40.9 ± 5.6	36.04 ± 3.0
≥9 T2 white matter lesions (%)	—	10 (58.8%)	6 (35.3%)	—	—
Dissemination in space Barkhof criteria (%)	—	11 (64.7%)	15 (88.2%)	11 (100%)	4 (66.6%)
Dissemination in space Swanson criteria (%)	—	17 (100%)	17 (100%)	—	—
Spinal cord lesions on MRI	—	10 (58.8%)	17 (100%)	—	—
Abnormal cerebrospinal fluid (%) [†]	—	12 (70.5%)	4 (23.5%) [‡]	1/4 [§]	3/1 [§]
Dissemination in time criteria	—	4 (23.5%)	5 (29.4%)	2 (16.6%)	3 (50.0%)
Gadolinum-enhancing lesions	—	0 (0%)	3 (17.6%)	0 (0%)	3 (50.0%)
Expanded Disability Status Scale total score	—	0 (0–1)	—	—	—
Vocabulary (WAIS-III)	46.7 ± 6.5	46.5 ± 6.6	44.5 ± 7.7	44.4 ± 7.7	18.5 ± 4.2
Matrix reasoning (WAIS-III)	16.6 ± 5.2	17.9 ± 3.2	17.3 ± 4.5	16.6 ± 4.8	44.8 ± 8.3
Hamilton Depression Rating Scale-17 total score [¶]	4.3 ± 4.9 (22.2%)	10.3 ± 6.9* (52.9%)	9.6 ± 7.2 (52.9%)	8.45 ± 7.1 (45.5%)	11.7 ± 7.5 (66.7%)
Failure on ≥1 cognitive tests (%) [#]	—	8 (47.1%)	8 (47.1%)	6 (54.5%)	2 (50%)
Failure on ≥2 cognitive tests (%) [#]	—	1 (5.9%)	2 (11.8%)	1 (9.1%)	1 (25%)
Volumetric assessment					
Normalized brain volume (×10 ³ cm ³)	1575 ± 36.8	1541 ± 66.6	1528 ± 64.4	1526 ± 72.7	1533 ± 51.49
Normalized cortical volume (×10 ³ cm ³)	673 ± 27.1	648 ± 27.3	641 ± 35.8**	643 ± 41.9	638 ± 24.3
Normalized gray matter volume (×10 ³ cm ³)	840 ± 35.7	828 ± 38.6	813 ± 38.5	814 ± 43.7	811 ± 30.4
Normalized white matter volume (×10 ³ cm ³)	731 ± 24.5	725 ± 42.8	715 ± 36.9	711 ± 39.2	722 ± 34.6
T2-white matter lesion volume (×10 ³ cm ³) ⁺	0.5 (0.1–0.9)	1.3 (0.7–3.7)	3.5 (1.2–6.4)	3.48 (1.7–4.6)	4.1 (0.8–11)

Mean ± standard deviation (range) and frequency (%) are reported. RIS = radiologically isolated syndrome, RISK+ = patients with radiologically isolated syndrome with higher risk for conversion to future multiple sclerosis, RISK – = patients with radiologically isolated syndrome with lower risk for conversion to future multiple sclerosis, WAIS-III = Wechsler Adult Intelligence Scale—Third Edition.

* *P* < 0.05 vs healthy controls.

** *P* < 0.01 vs healthy controls (Tukey test post hoc comparisons). Significant values are in bold font.

† Positive oligoclonal bands or an elevated immunoglobulin G index.

‡ Seven of 17 (41.2%) patients did not agree to undergo lumbar puncture.

§ Presence/absence of abnormal cerebrospinal fluid.

|| Ordinal variables or variables that were not normally distributed and therefore median (interquartile range) is provided.

¶ % of patients with clinically significant depression.

% of patients with abnormalities on cognitive tests.

TABLE 2. Normalized* Deep Gray Matter and Cerebellum Volumes (mm³) in Radiologically Isolated Syndrome and Clinically Isolated Syndrome Patients Compared With Healthy Controls

	Healthy Controls (N = 17)	Clinically Isolated Syndrome Patients (N = 17)	Radiologically Isolated Syndrome Patients (N = 17)	Group Differences (F [†] /P)
Deep gray matter volumes [‡]				
Mean thalamic	0.0051 ± 0.4	0.0047 ± 0.7	0.0046 ± 0.4[§]	4.61 / 0.018
Mean caudate	0.0025 ± 0.3	0.0025 ± 0.3	0.0024 ± 0.2	1.17 / 0.32
Mean putamen	0.0036 ± 0.2	0.0035 ± 0.5	0.0033 ± 0.4	0.95 / 0.40
Mean pallidum	0.0010 ± 0.1	0.0010 ± 0.1	0.0009 ± 0.1	1.33 / 0.28
Mean hippocampus	0.0029 ± 0.3	0.0029 ± 0.3	0.0028 ± 0.2	0.17 / 0.84
Mean amygdala	0.0011 ± 0.1	0.0010 ± 0.1	0.0009 ± 0.1	2.91 / 0.07
Mean cerebellum	0.035 ± 0.003	0.035 ± 0.004	0.033 ± 0.002	1.25 / 0.30

Mean ± standard deviations are reported. Significant values are in bold font.

* Normalized volume = volume mm³/total intracranial volume in mm³ (using FreeSurfer).

‡ Mean volumes were quantified as average of the 2 sides (left and right).

† Welch F-test for ANOVA.

§ P < 0.05 vs healthy controls.

cortex were found significantly reduced bilaterally. After Bonferroni correction for multiple comparisons was applied ($P < 0.0015$), no significant thinning differences were found between groups in any regional cortical area.

Strong inverse correlations were observed between T2-white matter lesion volume and regional cortical thickness (rho spearman ranging from 0.5 to 0.78).

In comparison to the widespread cortical thickness differences between the RIS and healthy controls, those from the CIS and healthy controls were very limited (Table 3).

DTI

Voxel-based analysis results obtained using fractional anisotropy maps are illustrated in figure. Note that the clusters with altered microstructural integrity overlap with lesion mask are dominant in both cuneate gyri (Figure 1A) and in bilateral frontal sub-gyral regions of RIS patients (Figure 1B) ($P < 0.001$). A significant fractional anisotropy decrease in cerebellum white matter was found among CIS patients ($P < 0.001$). No significant fractional anisotropy or mean diffusivity changes was found in the normal-appearing gray matter of both RIS and CIS patients when compared with healthy controls. Detailed results, including T-maps values, number of voxels in each cluster, Montreal Neurological Institute coordinates, and P values are presented in Table 4.

DISCUSSION

Damage to both the normal-appearing white matter and gray matter has increasingly been recognized as a crucial component of MS.^{33–35} Motivated by the scant information regarding gray matter pathology in RIS patients, we investigated whether gray matter involvement occurs in RIS patients and whether it shares anatomical patterns with CIS patients by using multimodal 3T MRI approach.

In line with the findings of a recent RIS study performed using the same method of analysis,¹⁰ we found significant mean thalamic volume loss in RIS patients compared with healthy controls. This is consistent with previous research that showed that thalamic volume loss is one of the earliest and most prominent signs of gray matter pathology in MS.^{36–38} This

finding might have a great clinical significance, as thalamic atrophy has been found as an independent predictor of the conversion to definite MS in patients with CIS.^{39,40} In the present study, thalamic atrophy was unrelated to the presence of other markers of evolution to MS. Future longitudinal studies are warranted to address whether thalamic atrophy in RIS patients may herald reliably the conversion to future MS. Unexpectedly, thalamic volume loss was more pronounced in RIS patients than in CIS patients. Thalamic atrophy, which has been shown to strongly correlated to white matter lesion volume,^{41,42} has been found primarily in those CIS patients who developed definite MS after a follow-up of 1 year.³⁸ In contrast, CIS patients from our cohort, many of whom have a disease duration >12 months, have not yet developed definite MS and are characterized by median low white matter lesion volume, which certainly might contribute to the explanation of the current results.

RIS patients also exhibited significantly reduced total normalized cortical volume and regional cortical atrophy compared with healthy controls. Furthermore, the most striking finding of the present study was that both global cortical volume and regional cortical thickness were more pronounced in RIS patients than in CIS patients. Although these results were somewhat unexpected, they are indeed in line with previous research. Thus, although a large number of studies did not find decreased whole brain and cortical volumes in CIS patients,^{36,37,39,43–45} all the studies published so far (with the exception of one publication)¹⁰ have reported total brain and cortical atrophy in RIS patients,^{3,6,8,9,12} thereby suggesting that, in contrast to CIS patients, decreased cortical volume in RIS patients is highly consistent. However, there are also several reasons that might partially explain these results: CIS patients had a lower median white matter lesion volume compared with RIS (albeit not significant); although there was no significant age difference among CIS and RIS groups in the present study, RIS patients were approximately 2 years older than those from the CIS group; nearly one-third of the CIS patients presented with spinal cord symptoms, which might lead to lower average cortical thickness (the type of clinical picture at onset has been found to correlate with atrophy in the corresponding cortical areas)⁴⁶; in contrast with MS and CIS patients, the absence of a

TABLE 3. Cortical Areas Showing Significant Cortical Thinning in Radiologically Isolated Syndrome and Clinically Isolated Syndrome Patients Compared With Healthy Controls

Cortical Area	Healthy Controls (N = 17)	Clinically Isolated Syndrome Patients (N = 17)	Radiologically Isolated Syndrome Patients (N = 17)	% Change	Number of Patients (%)**	Group Differences (F/P)
Global brain lobes cortical thickness*						
Right temporal lobe	3.07 ± 0.09 (2.93–3.26)	2.99 ± 0.14 (2.71–3.21)	2.94 ± 0.17 (2.65–3.19) †	4.53%	8 (47.1%)	3.40 / 0.04
Right cingulate cortex	2.59 ± 0.10 (2.46–2.78)	2.47 ± 0.10 (2.32–2.66) ‡	2.46 ± 0.13 (2.26–2.71) §	5.02%	6 (35.3%)	6.78 / 0.003
Left frontal lobe	2.55 ± 0.08 (2.43–2.69)	2.52 ± 0.07 (2.39–2.66)	2.47 ± 0.10 (2.33–2.64) ‡	3.13%	4 (23.5%)	4.07 / 0.02
Left cingulate cortex	2.55 ± 0.12 (2.35–2.81)	2.53 ± 0.06 (2.41–2.63)	2.45 ± 0.12 (2.20–2.68) ‡	3.92%	2 (11.8%)	4.39 / 0.02
Right hemisphere						
Rostrol gyrus	2.35 ± 0.07 (2.23–2.53)	2.32 ± 0.07 (2.24–2.54)	2.27 ± 0.09 (2.10–2.43) ‡	3.40%	26 (35.3%)	4.08 / 0.02
Lateral orbitofrontal	2.59 ± 0.14 (2.30–2.83)	2.52 ± 0.11 (2.39–2.75)	2.45 ± 0.13 (2.21–2.67) §	5.40%	3 (17.6%)	5.01 / 0.01
Superior temporal gyrus	2.95 ± 0.11 (2.81–3.17)	2.84 ± 0.17 (2.52–3.18)	2.82 ± 0.15 (2.57–3.08) ‡	4.40%	5 (29.4%)	3.78 / 0.03
Middle temporal gyrus	2.97 ± 0.08 (2.82–3.14)	2.88 ± 0.14 (2.65–3.18)	2.85 ± 0.16 (2.55–3.15) ‡	4.04%	6 (35.3%)	3.30 / 0.04
Transverse gyrus	2.68 ± 0.16 (2.43–2.95)	2.59 ± 0.19 (2.28–2.95)	2.45 ± 0.22 (2.03–2.82) §	8.58%	5 (29.4%)	5.79 / 0.006
Temporal pole	3.95 ± 0.21 (3.50–4.34)	3.85 ± 0.25 (3.49–4.38)	3.72 ± 0.29 (3.28–4.17) ‡	5.82%	5 (29.4%)	3.45 / 0.04
Caudal anterior cingulate	2.57 ± 0.12 (2.37–2.75)	2.43 ± 0.19 (2.16–2.82) ‡	2.41 ± 0.15 (2.05–2.65) §	6.22%	4 (23.5%)	5.62 / 0.006
Posterior cingulate	2.49 ± 0.10 (2.33–2.67)	2.42 ± 0.09 (2.27–2.60) ‡	2.40 ± 0.13 (2.19–2.62) ‡	3.61%	4 (23.5%)	3.34 / 0.04
Left hemisphere						
Pars triangularis	2.44 ± 0.08 (2.30–2.63)	2.41 ± 0.07 (2.27–2.57)	2.34 ± 0.13 (2.12–2.69) §	4.09%	6 (35.3%)	4.97 / 0.01
Pars orbitalis	2.74 ± 0.13 (2.41–2.92)	2.60 ± 0.13 (2.38–2.80) §	2.61 ± 0.17 (2.29–2.94) ‡	4.74%	5 (29.4%)	4.99 / 0.01
Lateral orbitofrontal	2.58 ± 0.10 (2.40–2.80)	2.53 ± 0.14 (2.37–2.82)	2.46 ± 0.10 (2.28–2.1) ‡	4.65%	4 (23.5%)	3.99 / 0.02
Inferior temporal gyrus	2.90 ± 0.13 (2.58–3.17)	2.82 ± 0.16 (2.60–3.11)	2.73 ± 0.18 (2.46–3.15) ‡	8.50%	7 (41.2%)	4.38 / 0.01
Fusiform gyrus	2.81 ± 0.10 (2.56–3.02)	2.76 ± 0.17 (2.52–3.13)	2.68 ± 0.17 (2.34–2.95) ‡	4.62%	5 (29.4%)	3.34 / 0.04
Transverse gyrus	2.59 ± 0.20 (2.25–2.90)	2.59 ± 0.19 (2.32–2.91)	2.40 ± 0.19 (2.11–2.70) †	7.33%	4 (23.5%)	5.05 / 0.01
Posterior cingulate	2.50 ± 0.11 (2.19–2.65)	2.45 ± 0.08 (2.24–2.60)	2.39 ± 0.13 (2.09–2.62) ‡	4.00%	2 (11.2%)	3.92 / 0.02

% change: (a–b)/b × 100 where a is cortical thickness of radiologically isolated syndrome patients and b is cortical thickness of healthy controls. Significant values are in bold font.

* Global lobes cortical thickness was quantified as average of the thickness of all lobe cortical areas.

** Number (percentage) of radiologically isolated syndrome patients who were at least two standard deviations below the healthy controls cortical thickness mean.

† P value for ANOVA group differences (uncorrected; adjusted for age and educational level).

‡ P < 0.05 vs healthy controls.

§ P < 0.01 vs healthy controls.

|| P < 0.05 vs clinically isolated syndrome patients.

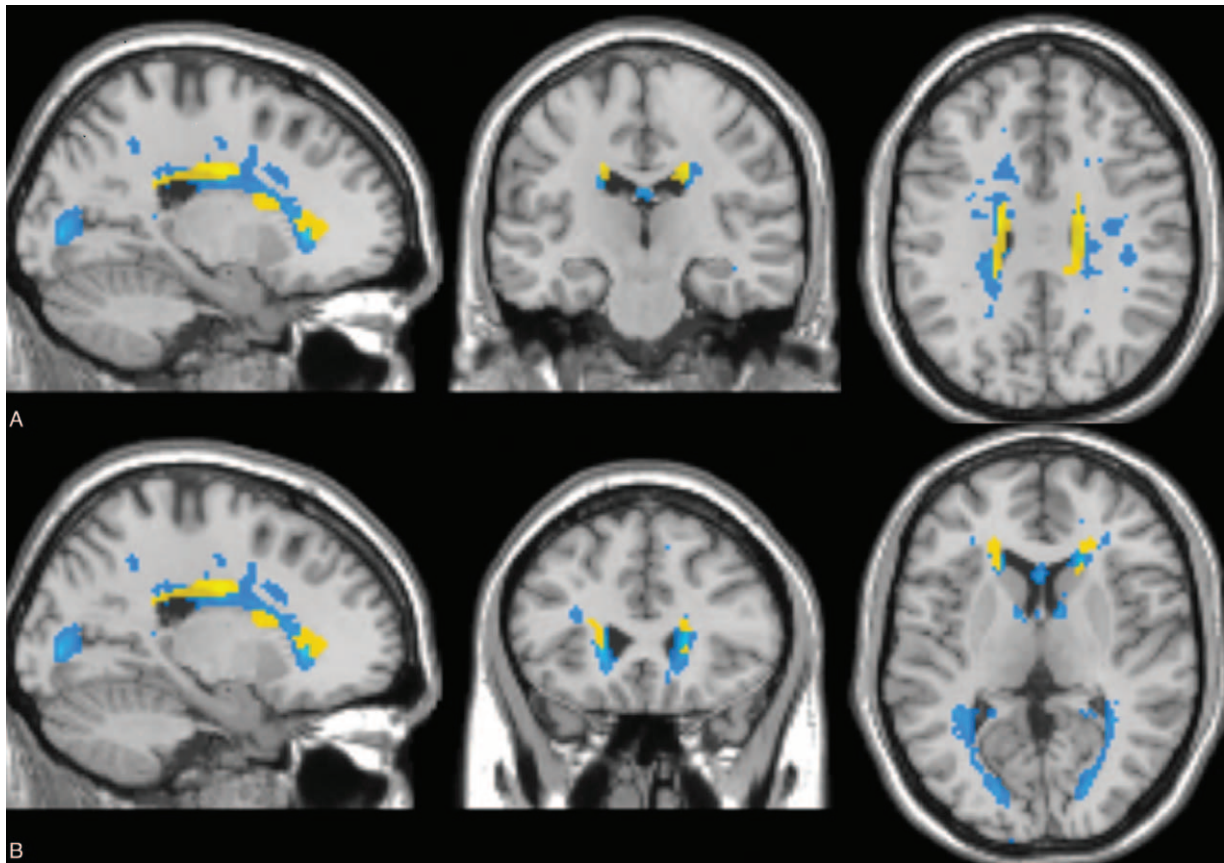


FIGURE 1. Voxel-based analysis results obtained using fractional anisotropy maps and mean lesion mask in radiologically isolated syndrome (RIS) patients. Sagittal, coronal, and axial views are presented. Clusters of reduced fractional anisotropy in RIS patients compared with healthy controls ($P < 0.001$) are shown in yellow and average lesion mask is shown in blue. The overlay of the significant map clusters on the mean lesion mask shows that most of the abnormalities highlighted by voxel-based analysis were primarily located within lesions. (A) Both cuneate gyri. (B) Bilateral frontal sub-gyral regions.

TABLE 4. Voxel-based Morphometry Analysis of Reduced Fractional Anisotropy in RIS Subjects Compared With Control Group

Voxel-based Analysis	T values	Number of Voxels in Each Cluster	Montreal Neurological Institute Coordinates (x, y, z)	P
Left hemisphere				
Frontal lobe sub-gyral	3.76	84	(-18, 32, 4)	<0.001
Cingulate gyrus	4.97	130	(-18, -12, 32)	<0.001
Cerebellum*	4.68	42	(-28, -66, -36)	<0.001
Right hemisphere				
Frontal lobe sub-gyral	3.94	151	(24, 34, 0)	<0.001
Cingulate gyrus	5.16	134	(18, -20, 30)	<0.001
Cerebellum*	4.02	12	(30, -66, -36)	<0.001

RIS = radiologically isolated syndrome.
* Clusters altered in clinically isolated syndrome patients.

definable clinical event makes it impossible to establish the disease evolution among RIS patients and, thus, there is the possibility that RIS evolution have actually a much longer duration than expected.

Although marginal and no significant cortical thinning was observed among CIS patients, RIS patients showed significant thinning in a number of cortical areas that were primarily distributed in frontal and temporal lobes, as well as cingulate cortex. Although the differences did not reach statistical significance after Bonferroni correction, their magnitudes were meaningful, as evidenced by the fact that most cortical areas were at least 2 SD below the healthy controls cortical thickness mean in one-third of the RIS patients. Furthermore, average right temporal lobe cortical thickness was significantly reduced in nearly half of the RIS patients. Although no differences were found among RIS patients with presence/absence of other markers of evolution to MS (eg, spinal cord lesions), the small sample size did not allow us to draw conclusions with regard to this issue.

Interestingly, we observed reduced cortical thickness in particular areas of great clinical relevance. First, regional significant atrophy were present in anterior cingulate cortex and orbitofrontal cortex, regions that have an established role in the pathophysiology of emotion processing and regulation.⁴⁷

Based on previous studies regarding clinical depression and its neurobiological basis,⁴⁸ we hypothesized that these findings could represent a structural brain trait factor for developing psychological disorders, thereby providing a plausible biological explanation for the high rates of psychiatric disturbances observed in RIS patients.⁴ Second, posterior cingulate cortex was found to be significantly thinner bilaterally. Posterior cingulate cortex is known to be commonly affected by neurodegenerative diseases and has recently been shown to be particularly thinner in long-standing MS patients.⁴⁹ In contrast, we did not observe cortical thickness in those brain regions that have been shown to play a critical role in motor function and physical dysfunction (precentral gyrus, sensorimotor cortex, and cerebellum), which contribute to explain why RIS patients subservise motor functions. Overall, these findings are totally in keeping with the clinical picture observed in RIS patients, characterized by null physical disability but high rates of cognitive and psychiatric disorders.^{4,5}

To our knowledge, only one study has investigated cortical thickness in RIS patients.¹⁰ In that study,¹⁰ a limited area of thinning in the right superior and inferior parietal gyri was observed by using vertex-wise map corrected for multiple comparisons. The possible explanations for these discrepant results are mainly methodological issues, such as the patients' characteristics at the study enrollment (no details about the presence of markers of evolution to MS or T2-white matter lesion volume were provided in the study of Azevedo),¹⁰ and the different statistical methods used to explore cortical thickness. In addition, 2 major problems inevitably related to RIS research might also contribute to find inconsistent results: the small sample sizes (an average of twenty patients) and the possibility that subjects fulfilling the RIS criteria actually constitute a highly heterogeneous group with different disease duration.

Another important finding of the present study is the observation that the voxel-based analysis did not reveal diffuse white matter fractional anisotropy or mean diffusivity changes in RIS patients. The results of the present study are in line with previous studies assessing microstructural integrity of white matter tracts in RIS patients by using magnetization transfer ratio⁶ and tract-based spatial statistics,¹² further suggesting that occult microstructural normal-appearing white-matter damage is not significant present beyond T2 visible lesions in RIS patients. These results suggest that RIS patients might have experienced more efficient reparative mechanisms after white matter injury, thereby contributing to explain the lack of episodes of neurologic disturbance existing in RIS patients.

Very recent studies have demonstrated that white matter microstructural integrity is the strongest predictor for regional cortical atrophy in MS patients.^{42,49,50} Therefore, although the lack of diffuse normal-appearing white matter damage might additionally contribute to explain the absence of global and regional cortical atrophy observed in CIS patients, it raises the question whether cortical atrophy in RIS patients develops according to a distinct pathological process than in MS disease. Indeed, regional cortical thinning in RIS patients showed stronger inverse correlation to white matter lesion volume than that reported in MS research. A new study specifically designed to assess the association between RIS regional gray matter atrophy and both focal and diffuse pathology in anatomically connected white matter tracts is in progress, which will be helpful to properly address this issue.

The study should be interpreted within the context of several limitations. First, the sample size was relatively small.

Given the low incidence and prevalence of the disease, the RIS literature generally comprises studies with small sample sizes.^{6–10,12} Second, we lacked for a method to visualize cortical lesions, the prevalence of which has been found to be as high as 40% among RIS patients,⁷ and, as a consequence, we were not able to assess their contribution to cortical thinning. However, cortical lesions in RIS patients have been shown not to be related to more pronounced cortical atrophy,⁷ which agrees with the conclusions of emerging research that suggest that cortical atrophy is largely independent of cortical demyelination.^{51–53} Third, MS lesions were not in-painted before submitting the image to FreeSurfer, which could compromise the accuracy of measured cortical thickness. However, according to a recent study,⁵⁴ lesion in-painting has only a small effect on the estimated regional and global cortical thickness. Fourth, The CIS group enrolled in the present study was not homogeneous in terms of disease duration from initial demyelinating event. Fifth, cerebrospinal fluid data were only available in a small proportion of RIS patients. Sixth, the regional cortical thickness results were not corrected for multiple comparisons, which lead to an increase in probability of observing significant comparison just due to chance. However, the magnitude of the differences is meaningful (one-third of RIS patients are at least 2 SDs below the healthy controls mean in most of the significant thinning regional areas). Moreover, such results were not observed in CIS patients, further strengthening our findings.

Being conscious of the limits of our study, RIS patients here described are currently enrolled in a longitudinal clinical and MRI study, which will be helpful in demonstrating more confident results. Notwithstanding, our results suggest the existence of neuronal degeneration in RIS patients regardless of the presence of an initial demyelinating clinical episode, highlighting that RIS brain tissue damage might not be limited to focal white matter lesions. Additional studies with larger sample sizes are warranted for a better understanding of the pathophysiological processes underlying this novel entity.

REFERENCES

- Okuda DT, Mowry EM, Beheshtian A, et al. Incidental MRI anomalies suggestive of multiple sclerosis: the radiologically isolated syndrome. *Neurology*. 2009;72:800–805.
- Lebrun C, Blanc F, Brassat D, et al., Cfsep. Cognitive function in radiologically isolated syndrome. *Multiple sclerosis*. 2010;16:919–925.
- Amato MP, Hakiki B, Goretti B, et al. Association of MRI metrics and cognitive impairment in radiologically isolated syndromes. *Neurology*. 2012;78:309–314.
- Labiano-Fontcuberta A, Aladro Y, Martinez-Gines ML, et al. Psychiatric disturbances in radiologically isolated syndrome. *J Psychiatr Res*. 2015;68:309–315.
- Labiano-Fontcuberta A, Martinez-Gines ML, Aladro Y, et al. A comparison study of cognitive deficits in radiologically and clinically isolated syndromes. *Multiple sclerosis*. 2015.
- De Stefano N, Stromillo ML, Rossi F, et al. Improving the characterization of radiologically isolated syndrome suggestive of multiple sclerosis. *PLoS one*. 2011;6:e19452.
- Giorgio A, Stromillo ML, Rossi F, et al. Cortical lesions in radiologically isolated syndrome. *Neurology*. 2011;77:1896–1899.
- Stromillo ML, Giorgio A, Rossi F, et al. Brain metabolic changes suggestive of axonal damage in radiologically isolated syndrome. *Neurology*. 2013;80:2090–2094.

9. Rojas JI, Patrucco L, Miguez J, et al. Brain atrophy in radiologically isolated syndromes. *Journal of neuroimaging: official journal of the American Society of Neuroimaging*. 2015;25:68–71.
10. Azevedo CJ, Overton E, Khadka S, et al. Early CNS neurodegeneration in radiologically isolated syndrome. *Neurol Neuroimmunol Neuroinflamm*. 2015;2:e102.
11. Okuda DT, Siva A, Kantarci O, et al. Radiologically isolated syndrome: 5-year risk for an initial clinical event. *PLoS one*. 2014;9:e90509.
12. Giorgio A, Stromillo ML, De Leucio A, et al. Appraisal of brain connectivity in radiologically isolated syndrome by modeling imaging measures. *J Neurosci*. 2015;35:550–558.
13. Barkhof F, Filippi M, Miller DH, et al. Comparison of MRI criteria at first presentation to predict conversion to clinically definite multiple sclerosis. *Brain: a journal of neurology*. 1997;120 (Pt 11):2059–2069.
14. Tintore M, Rovira A, Martinez MJ, et al. Isolated demyelinating syndromes: comparison of different MR imaging criteria to predict conversion to clinically definite multiple sclerosis. *AJNR American journal of neuroradiology*. 2000;21:702–706.
15. Kurtzke JF. Rating neurologic impairment in multiple sclerosis: an expanded disability status scale (EDSS). *Neurology*. 1983;33:1444–1452.
16. Gomez-Moreno M, Diaz-Sanchez M, Ramos-Gonzalez A. Application of the 2010 McDonald criteria for the diagnosis of multiple sclerosis in a Spanish cohort of patients with clinically isolated syndromes. *Multiple sclerosis*. 2012;18:39–44.
17. Swanton JK, Fernando K, Dalton CM, et al. Modification of MRI criteria for multiple sclerosis in patients with clinically isolated syndromes. *J Neurol Neurosurg Psychiatry*. 2006;77:830–833.
18. Rao SM, Leo GJ, Bernardin L, et al. Cognitive dysfunction in multiple sclerosis. I. Frequency, patterns, and prediction. *Neurology*. 1991;41:685–691.
19. Bondi MW, Serody AB, Chan AS, et al. Cognitive and neuropathologic correlates of Stroop Color-Word Test performance in Alzheimer's disease. *Neuropsychology*. 2002;16:335–343.
20. Kaufman AS, Lichtenberger EO. The essentials of WAIS-III assessment. New York; Chichester: J. Wiley; 1999.
21. de Oliveira MO, Nitrini R, Yassuda MS, et al. Vocabulary is an appropriate measure of premorbid intelligence in a sample with heterogeneous educational level in Brazil. *Behav Neurol*. 2014;2014:875960.
22. Hamilton M. A rating scale for depression. *J Neurol Neurosurg Psychiatry*. 1960;23:56–62.
23. Talairach J, Tournoux P. Co-planar stereotaxic atlas of the human brain; 3-dimensional proportional system: an approach to cerebral imaging. New York, N.Y.: Thieme Medical Publishers; 1988.
24. Fischl B, Salat DH, Busa E, et al. Whole brain segmentation: automated labeling of neuroanatomical structures in the human brain. *Neuron*. 2002;33:341–355.
25. Fischl B, Liu A, Dale AM. Automated manifold surgery: constructing geometrically accurate and topologically correct models of the human cerebral cortex. *IEEE Trans Med Imaging*. 2001;20:70–80.
26. Desikan RS, Segonne F, Fischl B, et al. An automated labeling system for subdividing the human cerebral cortex on MRI scans into gyral based regions of interest. *NeuroImage*. 2006;31:968–980.
27. Smith SM. Fast robust automated brain extraction. *Hum Brain Mapp*. 2002;17:143–155.
28. Maes F, Collignon A, Vandermeulen D, et al. Multimodality image registration by maximization of mutual information. *IEEE Trans Med Imaging*. 1997;16:187–198.
29. Ashburner J. A fast diffeomorphic image registration algorithm. *NeuroImage*. 2007;38:95–113.
30. Schmidt P, Gaser C, Arsic M, et al. An automated tool for detection of FLAIR-hyperintense white-matter lesions in Multiple Sclerosis. *NeuroImage*. 2012;59:3774–3783.
31. Smith SM, Zhang Y, Jenkinson M, et al. Accurate, robust, and automated longitudinal and cross-sectional brain change analysis. *NeuroImage*. 2002;17:479–489.
32. van Velsen EF, Vernooij MW, Vrooman HA, et al. Brain cortical thickness in the general elderly population: the Rotterdam Scan Study. *Neurosci Lett*. 2013;550:189–194.
33. Preziosa P, Rocca MA, Mesaros S, et al. Intrinsic damage to the major white matter tracts in patients with different clinical phenotypes of multiple sclerosis: a voxelwise diffusion-tensor MR study. *Radiology*. 2011;260:541–550.
34. Rovaris M, Riccitelli G, Judica E, et al. Cognitive impairment and structural brain damage in benign multiple sclerosis. *Neurology*. 2008;71:1521–1526.
35. Honce JM. Gray matter pathology in MS: neuroimaging and clinical correlations. *Mults Scler Int*. 2013;2013:627870.
36. Audoin B, Davies GR, Finisku L, et al. Localization of grey matter atrophy in early RRMS: A longitudinal study. *J Neurol*. 2006;253:1495–1501.
37. Henry RG, Shieh M, Okuda DT, et al. Regional grey matter atrophy in clinically isolated syndromes at presentation. *J Neurol Neurosurg Psychiatry*. 2008;79:1236–1244.
38. Rocca MA, Preziosa P, Mesaros S, et al. Clinically isolated syndrome suggestive of multiple sclerosis: dynamic patterns of gray and white matter changes: a 2-year MR imaging study. *Radiology*. 2016;278:841–853.
39. Calabrese M, Rinaldi F, Mattisi I, et al. The predictive value of gray matter atrophy in clinically isolated syndromes. *Neurology*. 2011;77:257–263.
40. Zivadinov R, Havrdova E, Bergsland N, et al. Thalamic atrophy is associated with development of clinically definite multiple sclerosis. *Radiology*. 2013;268:831–841.
41. Henry RG, Shieh M, Amirbekian B, et al. Connecting white matter injury and thalamic atrophy in clinically isolated syndromes. *J Neurol Sci*. 2009;282:61–66.
42. Steenwijk MD, Daams M, Pouwels PJ, et al. Unraveling the relationship between regional gray matter atrophy and pathology in connected white matter tracts in long-standing multiple sclerosis. *Hum Brain Mapp*. 2015;36:1796–1807.
43. Ceccarelli A, Rocca MA, Pagani E, et al. A voxel-based morphometry study of grey matter loss in MS patients with different clinical phenotypes. *NeuroImage*. 2008;42:315–322.
44. Raz E, Cercignani M, Sbardella E, et al. Clinically isolated syndrome suggestive of multiple sclerosis: voxelwise regional investigation of white and gray matter. *Radiology*. 2010;254:227–234.
45. Cappellani R, Bergsland N, Weinstock-Guttman B, et al. Diffusion tensor MRI alterations of subcortical deep gray matter in clinically isolated syndrome. *J Neurol Sci*. 2014;338:128–134.
46. Calabrese M, Atzori M, Bernardi V, et al. Cortical atrophy is relevant in multiple sclerosis at clinical onset. *J Neurol*. 2007;254:1212–1220.
47. Drevets WC, Price JL, Furey ML. Brain structural and functional abnormalities in mood disorders: implications for neurocircuitry models of depression. *Brain Struct Funct*. 2008;213:93–118.
48. Bora E, Fornito A, Pantelis C, et al. Gray matter abnormalities in Major Depressive Disorder: a meta-analysis of voxel based morphometry studies. *J Affect Disord*. 2012;138:9–18.

49. Steenwijk MD, Geurts JJ, Daams M, et al. Cortical atrophy patterns in multiple sclerosis are non-random and clinically relevant. *Brain*. 2016;139 (Pt 1):115–126.
50. Bergsland N, Lagana MM, Tavazzi E, et al. Corticospinal tract integrity is related to primary motor cortex thinning in relapsing-remitting multiple sclerosis. *Mult Scler*. 2015;21:1771–1780.
51. van de Pavert SH, Muhlert N, Sethi V, et al. DIR-visible grey matter lesions and atrophy in multiple sclerosis: partners in crime? *J Neurol Neurosurg Psychiatry*. 2015Apr 29. pii: jnnp-2014-310142. doi: 10.1136/jnnp-2014-310142. [Epub ahead of print].
52. Klaver R, Popescu V, Voorn P, et al. Neuronal and axonal loss in normal-appearing gray matter and subpial lesions in multiple sclerosis. *J Neuropathol Exp Neurol*. 2015;74:453–458.
53. Popescu V, Klaver R, Voorn P, et al. What drives MRI-measured cortical atrophy in multiple sclerosis? *Mult Scler*. 2015;21:1280–1290.
54. Govindarajan KA, Datta S, Hasan KM, et al. Effect of in-painting on cortical thickness measurements in multiple sclerosis: A large cohort study. *Hum Brain Mapp*. 2015;36:3749–3760.